7. ANKARA INTERNATIONAL AEROSPACE CONFERENCE AIAC-2013-014
11-13 September 2013 - METU, Ankara TURKEY

NUMERICAL SIMULATION OF FLUID STRUCTURE INTERACTION (FSI) EFFECT ON AN AIRCRAFT WING

Bhuiyan Shameem Mahmood Ebna Hai*
Helmut Schmidt University,
University of the Federal Armed Forces Hamburg
Holstenhofweg 85, 22043 Hamburg, Germany

ABSTRACT

Advanced composite materials are being applied to many aircraft structures to improve performance and reduce weight. However, aircraft wings can break due to Fluid-Structure Interaction (FSI) oscillations or material fatigue. The airflow around an airplane wing causes the wing to deform. While a wing deformation causes a change in the air pattern around it. Thrust force, turbulent flow and high speed, FSI plays an important role and complex mechanical effects are aroused. But due to nonlinear properties of fluid, material and shape of the structures, only numerical approaches can be used to solve such problems. This paper focuses on the analysis of a non-linear FSI problem and its solution in the finite element software package `DOpElib`: the `deal.II` based optimization library. The principal aim of this research is to explore and understand the behaviour of the FSI during the impact of a deformable material (of aircraft wing) on air. We briefly describe the analysis of Navier-Stokes and Elastodynamics equations in the Arbitrary Lagrangian-Eulerian (ALE) frameworks. This coupled problem is defined in a monolithic framework and fractional-step-θ time stepping scheme are implemented. Spatial discretization is based on a Galerkin finite element scheme. The non-linear system is solved by a Newton like method with different configurations.

Keywords: *Fluid-structure interaction (FSI), Arbitrary Lagrangian-Eulerian (ALE) frameworks, Navier-Stokes equations, Elastodynamic equations, Finite Element Method (FEM), Lift, Drag, Vibration,* ***`DOpElib`****,* ***`deal.II`****.*

NOMENCLATURE

$\widehat{\Omega}$	A bounded reference domain of the fluid structure interaction problem at time $t = 0$	Ω	A bounded domain of the fluid structure interaction problem, when $t > 0$
$\widehat{\rho}(\widehat{x})$	Lagrangian material density	$\rho(x,t)$	Eulerian density
μ	Dynamic viscosity	λ	Volumetric or bulk viscosity
ν_s	Poisson ratio	E_{Y_s}	Young modulus
p	hydrostatic pressure	σ_f	Cauchy stress tensor
λ	Volumetric or bulk viscosity	μ	Dynamic viscosity
$\widehat{u}_s$	Displacement of solid structure	v	Velocity of object
c	Velocity of sound	M_a	Mach Number
F_S	Surface forces	F_V	Volume forces
f	suffixe indicate fluid related terms	s	suffixe indicate structure related terms
$L^p(X)$	Banach space	$W^{m,p}(X)$	Sobolev space
$H^m(X)$	Hilbert space	$L^2(X)$	Lebesque space
V_X^*	Dual of V_X		

*Research fellow (Wissenschaftliche Mitarbeiter), Department of Mechanical Engineering, Email: ebnahaib@hsu-hh.de

INTRODUCTION

Currently, in various fields of engineering fluid-structure interactions (FSI) problems, become an important issue. However, due to the nonlinear properties of fluids and solids as well as the shape of the structures, only numerical approaches can be used to solve such problems. Simulation of the fluid-structure interaction, where the dynamics of these currents dominate, poses a formidable challenge for even the most advanced numerical techniques and is currently at the forefront of ongoing work in computational fluid dynamics.

Fluid-structure interactions (FSI) is interactions of some movable or deformable structure with an internal or surrounding fluid flow, which describe the coupled dynamics of fluid mechanics and structure mechanics. These types of problems are known as classical multi-physics problems. The problems can be stable or oscillatory. In this research work, we will focus on the analysis of the incompressible Navier-Stokes and elastodynamic equations in the arbitrary Lagrangian-Eulerian (ALE) frameworks and present a numerical simulation of the FSI effect on a double wedge airfoil, in which these equations shall describe the underlying physics. There are several interesting formulations of the equations for fluid, generally the Navier-Stokes equations, and for the equations for structure that are derived from the general theory of elasticity. In some cases, these equations are simplified with the use of models (e.g. turbulence models, wall functions, linear elastic material, etc.) or hypotheses (e.g. incompressible fluid, inviscid fluid, small strain, etc.) in order to reduce the complexity of the equations to be solved. For numerical approximation, these equations must be discretized using methods such as Finite Element (FE), Finite Volume (FV) or Finite Difference (FD), and an obtained system of discrete equations will be solved on a computer or computer cluster.

For the implementation, we chose `deal.II` [Bangerth, Heister and Kanschat] based software package `DOpElib` [Goll, Wick and Wollner]. While widely used commercial codes, e.g. NASTRAN, FLUENT, ANSYS or COMSOL Multiphysics, can only solve particular problems of aeroelasticity and hydroelasticity and are mainly limited to linearized models, `DOpElib` is a flexible toolbox providing modularized high-level algorithms that can be used to solve stationary and non-stationary PDE problems as well as optimal control problems constrained by PDEs. However, FSI problems introduce new complications and complexities to be considered, such as coupling techniques, dynamic interaction, different length and time scales of subsystems, therefore making these problems much more difficult than the seperate computation of the fluid and structure. Professors Rolf Rannacher, Thomas Dunne, Thomas Richter and their research groups introduced several interesting numerical techniques for solving the FSI benchmark example (see [Galdi and Rannacher , 2010; Bungartz and Schaefer , 2006; Bungartz, Miriam and Schaefer , 2010]). But there is not enough reference papers for study the FSI effect on an aircraft wing. With this in mind, and due to the challenge that it represents, the objective of this work is to contribute to the expansion of knowledge of this specific area.

MATHEMATICAL MODELS FOR FSI PROBLEMS IN ALE FRAMEWORK

Let us assume that $\widehat{\Omega} \subset \mathbb{R}^d, d = 2$ be a bounded domain of the fluid-structure interaction problem in reference configuration at time $t = 0$ with the Lipschitzian boundary [Bangerth and Rannacher , 2003; Hinze , 2011; Wollner , 2011]. The outer unit normal vector at the boundary is denoted by n. Assume that $\Omega := \Omega(t)$ is split into two time-dependent subdomains $\Omega_f(t)$ (for an incompressible fluid flow) and $\Omega_s(t)$ (for an elastic structure), which is slicked to at the boundary of the domain $\widehat{u}_s = 0$. Here, the boundaries of Ω, Ω_f and Ω_s are denoted by $\partial\Omega$, $\partial\Omega_f$ and $\partial\Omega_s$, respectively.

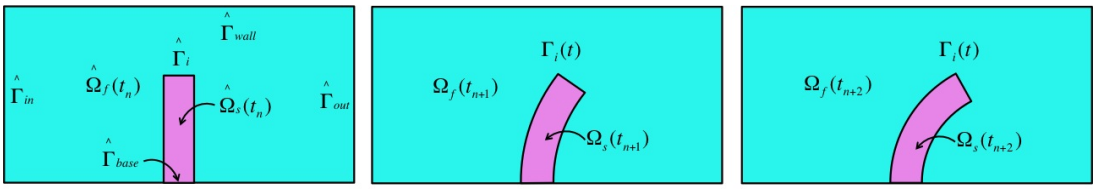

Figure 1: Typical FSI configuration

Due to the coupled dynamics of fluid and structure, the solid domain will be deformed $\widehat{\Omega}_s \mapsto \Omega_s(t)$ which also imposes a deformation of the flow domain $\widehat{\Omega}_f \mapsto \Omega_f(t)$. We split the boundary of $\widehat{\Omega}$ into the Dirichlet part $(\Gamma_D = \Gamma_{in} \cup \Gamma_{wall} \cup \Gamma_{base})$ and into the outflow (Neumann) boundary (Γ_{out}) as follows: $\partial\widehat{\Omega} = \Gamma_D \cup \Gamma_{out}$.

Since these boundaries do not move with time, Lagrangian and Eulerian coordinates coincide here. Fur-

thermore, in Eulerian and Lagrangian coordinates, the interface between both domains is denoted by $\Gamma_i(=\partial\widehat{\Omega}_f \cap \partial\widehat{\Omega}_s)$, which can move in time, i.e. $\Gamma_i(t) = \partial\Omega_f(t) \cap \partial\Omega_s(t)$. For convenience, the explicit time-dependence term is omitted and $\Omega := \Omega(t)$ is used to indicate time-dependent domains.

Functional spaces

Let us assume $X \subset \mathbb{R}^d, d = 2$ to be a time-independent domain where X can be used as $X := \Omega_f$ or $X := \Omega_s$. We know that $L^p(X), 1 \leq p \leq \infty$ indicate the standard Lebesgue space [Hinze , 2011; Wollner , 2011] that consists of measurable functions u, which are Lebesgue-integrable to the p-th power. The set $L^p(X)$ forms a Banach space [Hinze , 2011; Wollner , 2011] with the norm $|u|_{L^p(X)}$. The Sobolev space [Hinze , 2011; Wollner , 2011] $W^{m,p}(X), m \in N, 1 \leq p \leq \infty$ is the space of functions in $L^p(X)$ that have distributional derivatives of order up to m, which belong to $L^p(X)$.

For $p = 2, H^m(X) := W^{m,2}(X)$ is a Hilbert space equipped with the norm $\|.\|_{H^m(X)}$ [Wollner , 2011]. Finally, the subspace $W^{m,p}(X)$ of functions is indicated by $W_0^{m,p}(X)$ with zero trace on ∂X. Specifically, Hilbert space with zero trace on ∂X is defined as $H_0^1(X) = \{u \in H^1(X) : u|_{\Gamma_D} = 0,\ where\ \Gamma_D = \partial X_D\}$; ∂X_D is the part of the boundary ∂X at which Dirichlet boundary conditions are imposed.

A function $\wp \in L^2(X)$ has the weak or distributional derivative $u = \partial^\alpha \wp \in L^2(X)$ if $(\varphi, u)_X = (-1)^{|\alpha|}(\partial^\alpha \varphi, \wp)_X$ $\forall \varphi \in C_0^\infty(X)$ is satisfied, with the multi-index $\alpha = (\alpha_1, ..., \alpha_n)$, $\alpha_i \in \mathbb{N}_0$. Here, $|\alpha| := \alpha_1 + ... + \alpha_n$ and $\partial^\alpha := \partial^\alpha/(\partial^{\alpha_1}...\partial^{\alpha_n})$ and $C^\infty(X)$ denote the space of infinitely differentiable functions and $C_0^\infty(X)$ denotes a subspace whose elements are nonzero only on a subset of X.

So for a given set X, let us consider the Lebesque space $L_X := L^2(X)$ and $L_X^0 := L^2(X)/\mathbb{R}$. The functions in L_X with first-order distributional derivatives in L_X make up the Sobolev space $H^1(X)$. Furthermore, we can use the function spaces $V_X := H^1(X)^d$, $V_X^0 := H_0^1(X)^d$, and for time-dependent functions [Wick , 2011; Richter , 2010; Dunne , 2009]

$$\begin{aligned} \mathcal{L}_X &:= L^2[0,T;L_X], \qquad \mathcal{V}_X := L^2[0,T;V_X] \cap H^1[0,T;V_X^*], \\ \mathcal{L}_X^0 &:= L^2[0,T;L_X^0], \qquad \mathcal{V}_X^0 := L^2[0,T;V_X^0] \cap H^1[0,T;V_X^*], \end{aligned}$$

The Navier-Stokes equations in the Eulerian framework

Let us assume $\Omega_f \subset \mathbb{R}^d$ to be the domain with boundary $\Gamma_f = \partial\Omega_f$. Here, we can split this boundary into $\Gamma_f = \Gamma_{f_D} \cup \Gamma_{f_N}$, where Γ_{f_D} represents parts of the boundary with Dirichlet conditions and Γ_{f_N} the parts with Neumann boundary conditions. We then impose the boundary and initial values [Wick , 2011; Richter and Rannacher , 2010; Dunne and Rannacher , 2006]:

$$\begin{aligned} v_f(x,0) &= v_f^0 && \text{in } \Omega_f \\ v_f &= g && \text{on } \Gamma_{f_D} \subset \partial\Omega_f \\ \sigma_f.n_f &= [-p_f.I + 2\rho_f\nu_f\gamma(v_f)].n_f = h && \text{on } \Gamma_{f_N} \subset \partial\Omega_f \end{aligned}$$

where $g : \Gamma_{f_D} \times I \longmapsto \mathbb{R}^d$ and $h = h(x,t)$ are appropriate functions.

We derive the weak formulation of the Navier-Stokes equations in the Eulerian framework by multiplying with suitable test-functions. We introduce the following function spaces:

$$\begin{aligned} V_{\Omega_f}^0 &:= H_0^1(\Omega_f) = \{\phi^v \in H^1(\Omega_f)^d : v_f = 0 \ \text{ on } \Gamma_{f_D} = \partial\Omega_f\} \\ L_{\Omega_f}^0 &:= L_0^2(\Omega_f) = \{\phi^p \in L^2(\Omega_f) : (\phi^p, 1)_{\Omega_f} = 0\} \end{aligned}$$

and we get the variational formulation as:

Problem-1: The Navier-Stokes equations in the Eulerian framework:

Find $v_f \in v_f^D + V_{\Omega_f}^0$ and $p_f \in L_{\Omega_f}^0$ on $\Omega_f(t)$ such that the initial data satisfies $v_f(x,0) = v_f^0$ in Ω_f, and the following is true for almost all time steps $t \in I$:

$$\begin{aligned} (\nabla.v_f, \phi^p) &= 0 && \forall \phi^p \in L_{\Omega_f}^0 \\ (\rho_f(\partial_t v_f + (v_f.\nabla)v_f), \phi^v) & && \\ +(\mu_f\nabla v_f, \nabla\phi^v) - (\rho_f f_g, \phi^v) - \langle h, \phi^v\rangle_{\Gamma_{f_N}} &= 0 && \forall \phi^v \in V_{\Omega_f}^0 \end{aligned} \tag{1}$$

where, $\sigma_f := -p_f.I + 2\rho_f\nu_f\gamma(v_f) = -p_f.I + \rho_f\nu_f(\nabla v_f + \nabla v_f^T)$

However, in the case of a fluid-structure interaction, a Dirichlet condition is $v_f = v_s$ on the interface $\Gamma_i = \Gamma_f \cup \Gamma_s$ and the Neumann boundary conditions are mostly used for for the outflow boundary (do-nothing condition) i.e. a constant pressure on the outflow boundary.

Structure Mechanics

In this section, we shall describe the deformation and movement of an elastic structure domain $\widehat{\Omega}_s$ from the Lagrangian point of view. The displacement $\widehat{u}_s$ and mapping $\widehat{T}$, also referred to as the deformation $\widehat{T}(\widehat{x},t) = \widehat{x} + \widehat{u}(\widehat{x},t)$. The gradient of $\widehat{T}$ is the deformation gradient $\widehat{F} = \widehat{\nabla}\widehat{T}$. This work is concerned with numerical approximation of FSI effect on a St. Venant-Kirchhoff (STVK) compressible elastic material model. This model is suitable for large displacements with moderate strains.

The elasticity of material structures is characterized by the Poisson ratio ν_s and the Young modulus E_{Y_s}. The relationship of two material parameters μ_s and λ_s is given by [Galdi and Rannacher , 2010; Bungartz and Schaefer , 2006; Bungartz, Miriam and Schaefer , 2010]:

$$\nu_s = \frac{\lambda_s}{2(\lambda_s+\mu_s)}, \qquad E_{Y_s} = \mu_s\frac{3\lambda_s+2\mu_s}{\lambda_s+\mu_s}, \qquad \mu_s = \frac{E_{Y_s}}{2(1+\nu_s)}, \qquad \lambda_s = \frac{\nu_s E_{Y_s}}{(1+\nu_s)(1-2\nu_s)} \tag{2}$$

where for compressible material $\nu_s < \frac{1}{2}$ and incompressible material $\nu_s = \frac{1}{2}$.

Let us introduce the following function space:

$$\widehat{\mathcal{V}}^0_{\widehat{\Omega}_s} := H^1_0(\widehat{\Omega}_s;\widehat{\Gamma}_{s_D})^d = \{\phi \in H^1(\Omega_s)^d : \phi = 0 \ \text{ on } \ \widehat{\Gamma}_{s_D}\}$$

and we get the variational formulation of the structural equations in Lagrangian framework as [Richter , 2010; Dunne , 2009; Richter and Rannacher , 2010; Dunne and Rannacher , 2006]:

Problem-2: The Structural equations in Lagrangian framework:

Find $\widehat{u}_s \in \widehat{u}_s^D + \widehat{\mathcal{V}}^0_{\widehat{\Omega}_s}$ and $\widehat{v}_s \in \widehat{v}_s^D + \widehat{\mathcal{V}}^0_{\widehat{\Omega}_s}$ such that the initial data satisfies $\widehat{u}_s(\widehat{x},0) = \widehat{u}_s^0(\widehat{x})$ in $\widehat{\Omega}_s$, and for almost all time steps $t \in I$ holds:

$$\begin{aligned} (\widehat{v}_s,\widehat{\phi}^u) - \left(\partial_t\widehat{u}_s,\widehat{\phi}^u\right) = 0 \qquad & \forall\phi^u \in \widehat{V}^0_{\widehat{\Omega}_s} \\ \left(\widehat{\rho}_s\partial_t\widehat{v}_s,\widehat{\phi}^v\right) - (\widehat{J}\widehat{\sigma}_s\widehat{F}^{-T},\widehat{\nabla}\widehat{\phi}^v) & \\ -(\widehat{\rho}_s\widehat{f},\widehat{\phi}^v) - \langle\widehat{J}\widehat{\sigma}_s\widehat{F}^{-T},\widehat{\phi}^v\rangle_{\widehat{\Gamma}_{s_N}} = 0 \qquad & \forall\phi^v \in \widehat{V}^0_{\widehat{\Omega}_s} \end{aligned} \tag{3}$$

where,

$$\widehat{\sigma}_s = \frac{1}{\widehat{J}}\widehat{F}\left(2\mu_s\widehat{E} + \lambda_s tr(\widehat{E})I\right)\widehat{F}^T, \qquad \widehat{F}\widehat{S} = \widehat{F}\left(\lambda_s(tr(\widehat{E}))\widehat{I} + 2\mu_s\widehat{E}\right)$$

Here, the Dirichlet boundary conditions are built into the function space, and the Neumann condition on the stresses is given due to integration by parts.

The Navier-Stokes equations in the ALE framework

In fluid-structure interaction, the fluid flow problem is given on the moving domain $\Omega_f(t)$ and elastic structural system is given on the fixed domain $\widehat{\Omega}_s$, which can raise various problems. To avoid this, we want to formulate the flow problem on a fixed domain $\widehat{\Omega}_f$, where $\widehat{T}$ is a mapping between the fixed domain $\widehat{\Omega}_f$ and the moving domain Ω_f. Here, fluid's reference domain is arbitrary, and the structure will be formulated in Lagrangian co-ordinates, for which reason the resulting fluid-structure formulation is called the arbitrary Lagrangian Eulerian (ALE) formulation [Richter , 2010; Dunne , 2009].

Let it be assumed that $\widehat{T}_f : \widehat{\Omega}_f \longmapsto \Omega_f(t)$ is a C^2- diffeomorphism. We shall call $\widehat{T}_f$ the ALE mapping and define the gradient $\widehat{F}_f$ and its determinant $\widehat{J}_f$ by

$$\widehat{T}_f : \widehat{\Omega}_f \longmapsto \Omega_f(t), \qquad \widehat{F}_f := \widehat{\nabla}\widehat{T}_f, \qquad \widehat{J}_f := det(\widehat{F}_f)$$

The principle variables of velocity $\widehat{v}_f$ and pressure $\widehat{p}_f$ on the reference domain $\widehat{\Omega}_f$ shall be defined via the following transformation:

$$\widehat{v}_f(\widehat{x},t) = v_f(\widehat{T}_f(\widehat{x},t),t), \qquad \widehat{p}_f(\widehat{x},t) = p_f(\widehat{T}_f(\widehat{x},t),t)$$

Lemma-1:
Let $\widehat{T}_f : \widehat{\Omega}_f \longmapsto \Omega_f(t)$ be a C^1-diffeomorphism, $f \in H^1(\Omega_f(t))$ be a differentiable function and $u_f \in H^1(\Omega_f(t))^d$ a differentiable vector-field. The following it true for $\widehat{f}(\widehat{x},t) := f(x,t)$ and $\widehat{u}_f(\widehat{x},t) := u(x,t)$:

$$\partial_t f = \partial_t \widehat{f} - \left(\widehat{F}_f^{-1}\partial_t \widehat{T}_f.\widehat{\nabla}\right)\widehat{f}, \quad \nabla f = \widehat{F}_f^{-1}\widehat{\nabla}\widehat{f}, \quad (v_f.\nabla)f = \left(\widehat{F}_f^{-1}\widehat{v}_f.\widehat{\nabla}\right)\widehat{f}, \quad \nabla v_f = \widehat{\nabla}\widehat{v}_f\widehat{F}_f^{-1}.$$

Subsequently, by using divergence of the Piola transform theorem and Lemma-1, the variational formulation of the Navier-Stokes equations (see 1) on the moving domain $\Omega_f(t)$ can be mapped onto the reference domain [Richter , 2010] and we get:

Problem-3: The Navier-Stokes equations in ALE coordinates:

Let $\widehat{T}_f : \widehat{\Omega}_f \longmapsto \Omega_f(t)$ be a C^2 diffeomorphism. Consequently, the Navier-Stokes equations in artificial coordinates are given on $\widehat{\Omega}_f$ by finding $\widehat{v}_f \in \widehat{v}_f^D + \widehat{\mathcal{V}}^0_{\widehat{\Omega}_f}$ and $\widehat{p}_f \in \widehat{\mathcal{L}}_{\widehat{\Omega}_f}$, such that the initial data satisfiy $v_f(x,0) = v_f^0$ in Ω_f, and for almost all time steps $t \in I$ holds:

$$\begin{aligned}
\left(\widehat{div}(\widehat{J}_f\widehat{F}^{-1}\widehat{v}_f),\widehat{\phi}^p\right)_{\widehat{\Omega}_f} &= 0 \qquad \forall\widehat{\phi}^v \in \widehat{V}^0_{\widehat{\Omega}_f} \\
\left(\widehat{J}_f\widehat{\rho}_f\partial_t\widehat{v}_f,\widehat{\phi}^v\right)_{\widehat{\Omega}_f} + \left(\widehat{J}_f\widehat{\sigma}_f\widehat{F}_f^{-T},\widehat{\nabla}\widehat{\phi}^v\right)_{\widehat{\Omega}_f} & \\
+ \left(\widehat{J}_f\widehat{\rho}_f(\widehat{F}_f^{-1}(\widehat{v}_f - \partial_t\widehat{T}_f).\widehat{\nabla})\widehat{v}_f),\widehat{\phi}^v\right)_{\widehat{\Omega}_f} & \\
- \left(\widehat{J}_f\widehat{\rho}_f\widehat{f},\widehat{\phi}^v\right)_{\widehat{\Omega}_f} - \langle\widehat{h},\widehat{\phi}^v\rangle_{\widehat{\Gamma}_{f_N}} - \langle\widehat{J}_f\widehat{\sigma}_f\widehat{F}_f^{-T},\widehat{\phi}^v\rangle_{\widehat{\Gamma}_i} &= 0 \qquad \forall\widehat{\phi}^p \in \widehat{L}_{\widehat{\Omega}_f}
\end{aligned} \tag{4}$$

where $\widehat{\rho}_f$ is the density given on $\widehat{\Omega}_f$ and

$$\widehat{\sigma}_f(\widehat{x}) := -\widehat{p}_f I + \widehat{\rho}_f\nu_f\left(\widehat{\nabla}\widehat{v}_f\widehat{F}_f^{-1} + \widehat{F}_f^{-T}\widehat{\nabla}\widehat{v}_f^T\right), \qquad \widehat{F}_f := \widehat{\nabla}\widehat{T}_f, \qquad \widehat{J}_f := det\widehat{F}_f$$

If $\Omega = \widehat{\Omega}_f \cup \widehat{\Omega}_s$, we can formulate the fluid-structure interaction problem on one common domain. The interface $\widehat{\Gamma}_i = \widehat{\Omega}_f \cap \widehat{\Omega}_s$ is just the interface between both computational domains. Further, by solving the Navier-Stokes equations in ALE coordinates, the domain is fixed in time. Discretization is straightforward: we generate a triangulation $\widehat{\Omega}_{f,h}$ of $\widehat{\Omega}_f$ and can discretize with time stepping schemes in time and finite elements in space. The interface condition is given by

$$\widehat{v}_f(\widehat{x},t) = \widehat{v}_s(\widehat{x},t), \qquad \widehat{n}_f\left(\widehat{J}_f\widehat{\sigma}_f\widehat{F}_f^{-T}\right) + \widehat{n}_s\left(\widehat{J}_s\widehat{\sigma}_s\widehat{F}_s^{-T}\right) = 0 \quad \text{on } \widehat{\Gamma}_i$$

Let it be noted that even though the formulation looks just like the Lagrangian structure formulation, it must be stressed that the transformation $\widehat{T}_f$ is arbitrary and generally not the transformation to the Lagrangian coordinate system. Comparing the flow equations in ALE coordinates (Problem 3) with the Eulerian formulation in equation-1, we observe strong nonlinearities introduced by the transformation. In particular, its gradient $\widehat{F}_f$ enters into the equation in various ways. For the formulation to be well posed, it has to be at least invertible. Since this transformation will not be given analytically (because it will have to depend on the unknown solution itself to fit the structure's domain), this will give rise to serious problems.

The Fluid-Structure Interaction Problem in the ALE framework

The variational ALE formulation of the fluid part is transformed from its Eulerian description into an arbitrary Lagrangian framework and stated on the (arbitrary) reference domain $\widehat{\Omega}_f$, while the structure part is formulated in Lagrangian coordinates on the domain $\widehat{\Omega}_s$, where $\widehat{\Omega} = \widehat{\Omega}_f \cup \widehat{\Gamma}_i \cup \widehat{\Omega}_s$.

Moreover, here we solve the Laplace equation for the definition of the ALE mapping. Here, the continuity of velocity $\widehat{v}_f = \widehat{v}_s$ and $\widehat{u}_f = \widehat{u}_s$ across the common fluid-structure interface on $\widehat{\Gamma}_i = \widehat{\Omega}_f \cup \widehat{\Omega}_s$. We search for $\widehat{u} \in H^1(\widehat{\Omega}_f,\widehat{\Gamma}_D)^d$ and $\widehat{v} \in H^1(\widehat{\Omega}_f,\widehat{\Gamma}_D)^d$, where the local quantities are defined by restrictions:

$\widehat{v}_f := \widehat{v}|_{\widehat{\Omega}_f}$, $\widehat{v}_s := \widehat{v}|_{\widehat{\Omega}_s}$ and $\widehat{u}_s := \widehat{u}|_{\widehat{\Omega}_s}$.

Since there is no pressure variable given in the solid domain, we harmonically extend the fluid-pressure $\widehat{p}_f$ to $\widehat{\Omega}_s$. On all $\widehat{\Omega}$, we denote the pressure field by $\widehat{p}$.

It is noted that this extension of the pressure is an inconsistency. While the fluid's pressure is of low regularity $\widehat{p}_f \in L_0^2(\widehat{\Omega}_f)$, the Laplace equation yields $\widehat{p}_s \in H^1(\widehat{\Omega}_s)$. This additional regularity will feed back into the fluid domain if the extension is not properly decoupled. Since the ALE mapping is defined in accordance to the Lagrange-Euler structure mapping via $\widehat{T} := \widehat{x} + \widehat{u}_f$, we can define the following on all Ω: $\widehat{T} := \widehat{x} + \widehat{u}$, $\widehat{F} := I + \widehat{\nabla}\widehat{u}$, and $\widehat{J} := det(\widehat{F})$.

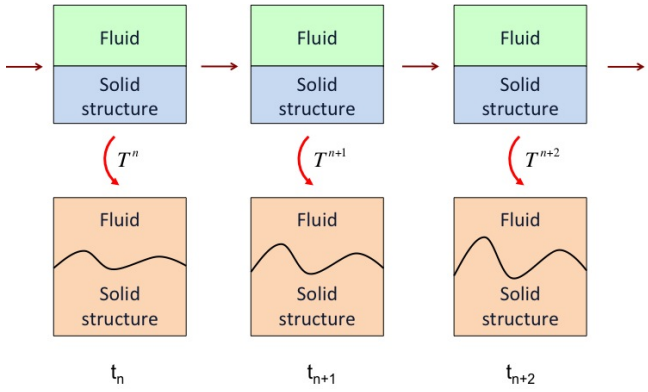

Figure 2: Typical FSI Problem in the ALE framework

In the structure domain, $\widehat{T}$ takes the place of the Lagrangian-Eulerian coordinate transformation, while in the fluid domain, $\widehat{T}$ has no physical meaning but serves as ALE mapping [Dunne , 2009; Wick , 2011].

Problem-4: The fluid-structure interaction problem in ALE framework: Find $\widehat{v} \in \widehat{v}^D + \widehat{\mathcal{V}}^0_{\widehat{\Omega}}$, $\widehat{u} \in \widehat{u}^D + \widehat{\mathcal{V}}^0_{\widehat{\Omega}}$ and $\widehat{p} \in \widehat{\mathcal{L}}_{\widehat{\Omega}}$, such that $\widehat{u}(0) = \widehat{u}^0$ and $\widehat{v}(0) = \widehat{v}^0$, for almost all time steps $t \in I$ holds:

$$
\begin{aligned}
&\left(\widehat{J}_f\widehat{\rho}_f\partial_t\widehat{v}_f, \widehat{\phi}^v\right)_{\widehat{\Omega}_f} + \left(\widehat{J}_f\widehat{\rho}_f(\widehat{F}_f^{-1}(\widehat{v}_f - \partial_t\widehat{T}_f).\widehat{\nabla})\widehat{v}_f), \widehat{\phi}^v\right)_{\widehat{\Omega}_f} \\
&\quad + \left(\widehat{J}\widehat{\sigma}_f\widehat{F}^{-T}, \widehat{\nabla}\widehat{\phi}^v\right)_{\widehat{\Omega}_f} - \langle\widehat{h}, \widehat{\phi}^v\rangle_{\widehat{\Gamma}_N} - \left(\widehat{J}\widehat{\rho}_f\widehat{f}_f, \widehat{\phi}^v\right)_{\widehat{\Omega}_f} \\
&+ \left(\widehat{\rho}_s\partial_t\widehat{v}, \widehat{\phi}^v\right)_{\widehat{\Omega}_s} - \left(\widehat{\rho}_s\widehat{f}_s, \widehat{\phi}^v\right)_{\widehat{\Omega}_s} - \left(\widehat{J}\widehat{\sigma}_s\widehat{F}^{-T}, \widehat{\nabla}\widehat{\phi}^v\right)_{\widehat{\Omega}_s} = 0 \qquad \forall\widehat{\phi}^v \in \widehat{V}^0_{\widehat{\Omega}} \qquad (5) \\
&\left(\widehat{div}(\widehat{J}\widehat{F}^{-1}\widehat{v}), \widehat{\phi}^p\right)_{\widehat{\Omega}_f} + \left(p_s, \widehat{\phi}^p\right)_{\widehat{\Omega}_s} = 0 \qquad \forall\widehat{\phi}^p \in \widehat{L}_{\widehat{\Omega}} \\
&\left(\partial_t\widehat{u} - v, \widehat{\phi}^u\right)_{\widehat{\Omega}_s} + \left(\widehat{\sigma}_g, \widehat{\nabla}\widehat{\phi}^u\right)_{\widehat{\Omega}_f} - \langle\widehat{\sigma}_g, \widehat{n}^f, \widehat{\phi}^u\rangle_{\widehat{\Gamma}_i} = 0 \qquad \forall\widehat{\phi}^u \in \widehat{V}^0_{\widehat{\Omega}}
\end{aligned}
$$

The stress tensors for the fluid and structure are implemented in $\widehat{\sigma}_f$, $\widehat{\sigma}_s$, and $\widehat{\sigma}_g$, where the stress tensors are given by

$$\widehat{\sigma}_f(\widehat{x}) = -p_f I + \widehat{\rho}_f\nu_f\left(\widehat{\nabla}\widehat{u}_f\widehat{F}_f^{-1} + \widehat{F}_f^{-T}\widehat{\nabla}\widehat{u}_f^T\right)$$
$$\widehat{\sigma}_s = \widehat{J}^{-1}\widehat{F}\left(2\mu_s\widehat{E} + \lambda_s tr(\widehat{E})I\right)\widehat{F}^T$$

In this formulation, for momentum equations, integration by parts in both subdomains yields the boundary term on $\widehat{\Gamma}_i$ as:

$$\left(\widehat{n}_f.(\widehat{J}\widehat{\sigma}_s\widehat{F}^{-T}), \widehat{\phi}^v\right)_{\widehat{\Gamma}_i} + \left(\widehat{n}_s.(\widehat{J}\widehat{\sigma}_f\widehat{F}^{-T}), \widehat{\phi}^v\right)_{\widehat{\Gamma}_i} = 0$$

Galerkin Formulation

For arguments $\widehat{U} = \{\widehat{v}, \widehat{u}, \widehat{p}\}$ and $\widehat{\Phi} = \{\widehat{\phi}^v, \widehat{\phi}^u, \widehat{\phi}^p\} \in \widehat{X}^0_D$, where $\widehat{X}^0_D := \{\widehat{v}^D + \widehat{\mathcal{V}}^0_{\widehat{\Omega}}\} \times \{\widehat{u}^D + \widehat{\mathcal{V}}^0_{\widehat{\Omega}}\} \times \widehat{\mathcal{L}}^0_{\widehat{\Omega}}$, we

introduce the space-time semilinear form-

$$\begin{aligned}\widehat{A}(\widehat{q},\widehat{U})(\widehat{\Phi}) = \int_0^T \{ &\Big(\widehat{J}_f\widehat{\rho}_f\partial_t\widehat{v}_f,\widehat{\phi}^v\Big)_{\widehat{\Omega}_f} + \Big(\widehat{J}\widehat{\sigma}_f\widehat{F}^{-T},\widehat{\nabla}\widehat{\phi}^v\Big)_{\widehat{\Omega}_f} \\ &+ \Big(\widehat{J}_f\widehat{\rho}_f(\widehat{F}_f^{-1}(\widehat{v}_f-\partial_t\widehat{T}_f).\widehat{\nabla})\widehat{v}_f),\widehat{\phi}^v\Big)_{\widehat{\Omega}_f} \\ &+ \Big(\widehat{div}(\widehat{J}\widehat{F}^{-1}\widehat{v}),\widehat{\phi}^p\Big)_{\widehat{\Omega}_f} - \Big(\widehat{J}\widehat{\rho}_f\widehat{f}_f,\widehat{\phi}^v\Big)_{\widehat{\Omega}_f} \\ &+ \Big(\widehat{\sigma}_g,\widehat{\nabla}\widehat{\phi}^u\Big)_{\widehat{\Omega}_f} + \Big(\widehat{\rho}_s\partial_t\widehat{v},\widehat{\phi}^v\Big)_{\widehat{\Omega}_s} \\ &+ \Big(p_s,\widehat{\phi}^p\Big)_{\widehat{\Omega}_s} - \Big(\widehat{J}\widehat{\sigma}_s\widehat{F}^{-T},\widehat{\nabla}\widehat{\phi}^v\Big)_{\widehat{\Omega}_s} - \Big(\widehat{\rho}_s\widehat{f}_s,\widehat{\phi}^v\Big)_{\widehat{\Omega}_s} \\ &+ \Big(\partial_t\widehat{u}-v,\widehat{\phi}^u\Big)_{\widehat{\Omega}_s} - \langle\widehat{h},\widehat{\phi}^v\rangle_{\widehat{\Gamma}_N} - \langle\widehat{\sigma}_g,\widehat{n}^f,\widehat{\phi}^u\rangle_{\widehat{\Gamma}_i}\}dt\end{aligned} \tag{6}$$

Problem-5: Compact ALE formulation of the FSI problem:

Find $\widehat{U}\in\widehat{U}^D+\widehat{\mathcal{X}}$, such that

$$\widehat{A}(\widehat{q},\widehat{U})(\widehat{\Phi})=0 \quad \forall\Phi\in\widehat{\mathcal{X}}^0 \tag{7}$$

where $\widehat{U}^D$ is an appropriate extension of the Dirichlet boundary and initial data, and the space $\widehat{\mathcal{X}}^0$ is defined by

$$\widehat{\mathcal{X}}^0 := \{\widehat{\Phi}\in\widehat{\mathcal{V}}^0_{\widehat{\Omega}}\times\widehat{\mathcal{V}}^0_{\widehat{\Omega}}\times\widehat{\mathcal{L}}^0_{\widehat{\Omega}_s},\widehat{\phi}^v(0)=\widehat{\phi}^u(0)=0\}$$

DISCRETIZATION

Time Discretization

The discretization in time is done by the well-known "fractional-step-θ scheme", where each time step $t_{n-1}\mapsto t_n$ is split into three substeps $t_{n-1}\mapsto t_{n-1+\theta}\mapsto t_{n-\theta}\mapsto t_n$.

We can formulate an abstract differential-algebraic equation (DAE) by fractional-step-θ scheme as [Richter and Rannacher , 2010; Wick , 2011; Dunne and Rannacher , 2006]:

$$\begin{bmatrix} M & 0\\ 0 & 0\end{bmatrix}\begin{bmatrix}\dot{v}(t)\\ \dot{p}(t)\end{bmatrix}+\begin{bmatrix} A(v(t)) & B\\ -B^T & C\end{bmatrix}\begin{bmatrix}\dot{v}(t)\\ \dot{p}(t)\end{bmatrix}=\begin{bmatrix} b(t)\\ c(t)\end{bmatrix} \tag{8}$$

which resembles the operator form of the spatially discretized incompressible Navier-Stokes equations with pressure stabilization. Let the parameters be $\theta=1-\frac{\sqrt{2}}{2}=0.292893...$, $\theta'=1-2\theta$, $\alpha\in(0.5,1]$, and $\beta=1-\alpha$, and the fractional-step-θ scheme can be reads as [Richter and Rannacher , 2010; Dunne and Rannacher , 2006]:

$$\begin{aligned}\begin{bmatrix} M+\alpha\theta kA^{n-1+\theta} & \theta kB\\ -B^T & C\end{bmatrix}\begin{bmatrix} v^{n-1+\theta}\\ p^{n-1+\theta}\end{bmatrix}&=\begin{bmatrix}[M-\beta\theta kA^{n-1}]v^{n-1}+\theta kb^{n-1}\\ c^{n-1+\theta}\end{bmatrix}\\ \begin{bmatrix} M+\beta\theta' kA^{n-\theta} & \theta' kB\\ -B^T & C\end{bmatrix}\begin{bmatrix} v^{n-\theta}\\ p^{n-\theta}\end{bmatrix}&=\begin{bmatrix}[M-\alpha\theta' kA^{n-1+\theta}]v^{n-1+\theta}+\theta' kb^{n-\theta}\\ c^{n-\theta}\end{bmatrix}\\ \begin{bmatrix} M+\alpha\theta kA^{n} & \theta kB\\ -B^T & C\end{bmatrix}\begin{bmatrix} v^{n}\\ p^{n}\end{bmatrix}&=\begin{bmatrix}[M-\beta\theta kA^{n-\theta}]v^{n-\theta}+\theta kb_h^{n-\theta}\\ c^{n}\end{bmatrix}\end{aligned} \tag{9}$$

where, $A^{n-1+\theta}:=A(x^{n-1+\theta})$, $b^{n-1}:=b(t_{n-1})$.

Here, the fractional-step-θ is second order scheme and has a similar work complexity to the Crank-Nicholson scheme, where $\alpha=\frac{1}{2}$. The fractional-step-θ scheme was originally proposed within each cycle $t_{n-1}\mapsto t_{n-1+\theta}\mapsto t_{n-\theta}\mapsto t_n$ in form of an operator splitting scheme separating the two complications "non-linearity" and "incompressibility".

In time-discretization, we introduce the mixed continuous Galerkin (cG(1)) method for velocity and deformation and for pressure, we consider a discontinuous Galerkin (dG(0)) method. Let the time interval $\overline{I}=[0,T]$ with $M\in\mathbb{N}$ subintervals be described as follows:

$$\overline{I}=\{0\}\cup I_1\cup I_2\cup....\cup I_M,$$

where $I_n = (t_{n-1}, t_n]$, $t_n > t_{n-1}$, and $k_n := t_m - t_{m-1}$.

Now we shall introduce the following two time-discrete spaces for the velocity and deformation:

$$\widehat{\mathcal{V}}_k^{cG} := \{v_k \in C(\overline{I}, \widehat{V})|_{v_k|I_n} \in P_1(I_n, \widehat{V}), n = 1, 2, ..., M\},$$
$$\widehat{\mathcal{V}}_k^{dG} := \{v_k \in L^2(I, \widehat{V})|_{v_k|I_n} \in P_0(I_n, \widehat{V}), n = 1, 2, ..., M, v_k(0) \in \widehat{V}_k\},$$

where $P_1(I, \widehat{V})$ and $P_0(I, \widehat{V})$ are the spaces of linear and constant functions, respectively, on I with values in $\widehat{V}$. Here, the time-discrete space $\widehat{\mathcal{V}}_k^{cG}$ contains continuous functions which are piecewise linear in time, and $\widehat{\mathcal{V}}_k^{dG}$ contains discontinuous and constant functions on every subinterval I_m.

For pressure, we define piecewise constant functions in time as:

$$\widehat{\mathcal{L}}_k^{dG} := \{p_k \in L^2(I, \widehat{L})|_{p_k|I_n} \in P_0(I_n, \widehat{L}), n = 1, 2, ..., M\}$$

Problem-6: Time discrete Galerkin approximation of the FSI problem in ALE formulation:

Find $\widehat{U}_k \in \widehat{U}_k^D + \widehat{\mathcal{X}}_k^{cG}$, such that

$$\widehat{A}(\widehat{q}_k, \widehat{U}_k)(\widehat{\Phi}_k) = 0 \quad \forall \Phi_k \in \widehat{\mathcal{X}}_k^{dG}. \tag{10}$$

where,

$$\widehat{\mathcal{X}}_k^{dG} := \widehat{\mathcal{V}}_k^{dG} \times \widehat{\mathcal{V}}_k^{dG} \times \widehat{\mathcal{L}}_k^{dG},$$
$$\widehat{\mathcal{X}}_k^{cG} := \widehat{\mathcal{V}}_k^{cG} \times \widehat{\mathcal{V}}_k^{cG} \times \widehat{\mathcal{L}}_k^{cG}$$

The test functions from $\widehat{\mathcal{X}}_k^{dG}$ are discontinuous in time, and this Galerkin scheme splits into a time-stepping method, where

$$v_k^n := v_k(t_n), \qquad u_k^n := u_k(t_n), \qquad p_k^n := p_k|I_n, \qquad \phi_k^n := \phi_k|I_n$$

Mesh Notation

In the Galerkin finite element method, the spatial discretization is conforming on meshes $\mathbf{T}_h$ consisting of N cells that are denoted by K.

$$\overline{\Omega} = \bigcup_{i=1,...,N} \overline{K}_i$$

where the mesh parameter h is a scalar cell-wise constant function and defined as $h|_K := h_K = diam(K)$ and with the assumption $h_{max} := \max_{K \in \mathbf{T}_h} h_k$. Here, $\mathbf{T}_h$ is considered "regular" if any cell edge is either a subset of the domain boundary components Γ_D, Γ_N or a complete face or edge of another cell.

To ensure proper approximation properties of the finite element spaces which are constructed based on the meshes $\mathbf{T}_h$, we require the following regularity condition to be fulfilled:

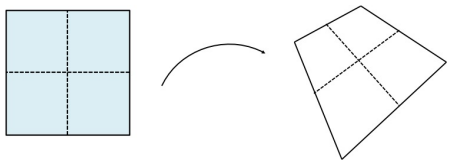

Figure 3: Reference mapping $\sigma_K : \widehat{K} \longmapsto K$

Mesh regularity condition: Each cell $K \in \mathbf{T}_h$ is the image of the reference unit cube $\widehat{K} = [0, 1]^d$ under some d-linear mapping $\sigma_K : \widehat{K} \longmapsto K$ (see Figure-3). This mapping is uniquely described by the 2^d coordinate values of the corners of K, if the ordering of the corners is preserved. The Jacobian tensors σ'_K of these mappings are invertible and satisfy the uniform bounds

$$\sup_{h>0} \max_{K \in \mathbf{T}_h} ||\sigma'_K|| \leq c$$
$$\sup_{h>0} \max_{K \in \mathbf{T}_h} ||(\sigma'_K)^{-1}|| \leq c$$

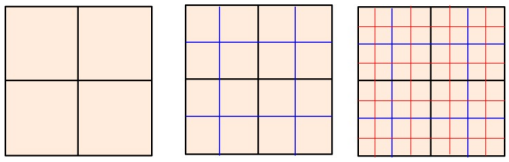

Figure 4: Global refinement: a regular mesh after two cycles

This condition is satisfied if the cells $K \in \mathbf{T}_h$ possess the usual structural properties of uniform "non-degeneracy", "uniform shape", and "uniform size property".

Now if we want to increase the number of cells in a decomposition of $\mathbf{T}_h$, we need to refer to "mesh refinement", which consists of subdividing a cell into 2^d sub cells. Connecting the midpoints of opposing faces or edges of a cell subdivides the cell. A refinement is "global" if this is done for every cell (see Figure-4), and it is called "local" if subdividing is done for some cells (see Figure-5).

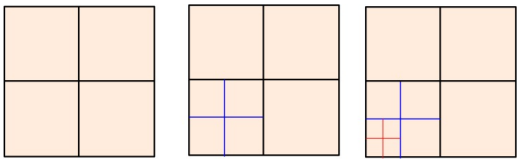

Figure 5: Local refinement: a regular mesh after two cycles

In the case of patch-wise local refinement, we require a decomposition of $\mathbf{T}_h$, which is the result of global refinement of the coarser decomposition of $\mathbf{T}_{2h}$, as shown in Figure-6.

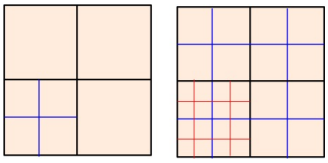

Figure 6: Patch-wise local refinement: a regular mesh after two cycles

Problem-7: Space-Time discrete Galerkin approximation of the FSI problem in ALE formulation:

Find $\widehat{U}_{kh} \in \widehat{U}^D_{kh} + \widehat{\mathcal{X}}^{cG}_{kh}$, such that $\widehat{A}(\widehat{q}_{kh}, \widehat{U}_{kh})(\widehat{\Phi}_{kh}) = 0$ for all $\Phi_h \in \widehat{\mathcal{X}}^{dG}_h$.

where the discrete finite element spaces $\widehat{\mathcal{X}}^{cG}_{kh}$ and $\widehat{\mathcal{X}}^{dG}_{kh}$ are defined analog as their continuous counterparts.

$$\begin{aligned}
\widehat{\mathcal{V}}^{cG}_{kh} &:= \{v_{kh} \in C(\bar{I}, \widehat{V})|_{v_{kh}|I_n} \in P_1(I_n, \widehat{V}_{mh}), n = 1, 2, ..., M\},\\
\widehat{\mathcal{V}}^{dG}_{kh} &:= \{v_{kh} \in L^2(\bar{I}, \widehat{V})|_{v_{kh}|I_n} \in P_0(I_n, \widehat{V}_{mh}), n = 1, 2, ..., M\},\\
\widehat{\mathcal{L}}^{dG}_{kh} &:= \{p_{kh} \in L^2(I, \widehat{L})|_{p_{kh}|I_n} \in P_0(I_n, \widehat{V}_{mh}), n = 1, 2, ..., M\}.
\end{aligned}$$

Here for $\widehat{\mathcal{V}}^{dG}_{kh}$, $v_{kh}(0) \in \widehat{V}_{0h}$.

NUMERICAL EXAMPLE

The aim of this research is to explore and understand the behaviour of engineering artefacts in extreme environments. To achieve the main ambition of this work, we split this research into two parts. The first part will consider to determine the effect of fluid flow over a sample airfoil (2D) and study the displacement of a control point $A(t)$ under incompressible fluid flow. The second part of this research focused on FSI effect on 3D aircraft wing to identify the list of critical design points to implementing a Damage Identification Strategy (DIS) [Ebna Hai and Bause , 2013], where we will design an integrated SHM system for an aircraft. But numerical simulations FSI on a sample aircraft wing (3D) still in progress.

Configuration test model

The computational domain is designed based on the $2D$ FSI benchmark as shown in Figure-7 and it is determined by following characteristics:

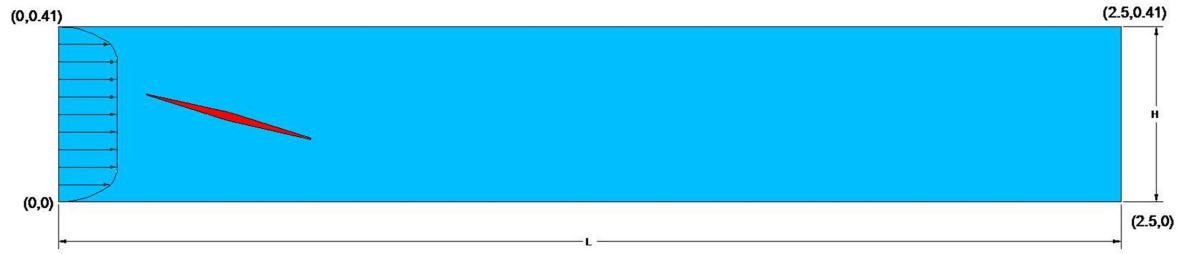

Figure 7: Computational domain

- The computational domain has the length $L = 2.5$ and height $H = 0.41$.
- We will examine a double wedge airfoil as our test model. The chord length of the airfoil $c = 0.41$ and maximum thickness $t = 0.07$ with a 15 degree angle of attack (AOA).
- Left end and right lower end of the airfoil is positioned at $(0.2, 0.253)$ and $(0.6, 0.147)$, respectively.
- The control points $A(t)$ are fixed at the trailing edge of the structure with $A(t)|_{t=0} = (0.6, 0.147)$, measuring x and y- deflections of the airfoil.

Material properties

The fluid is assumed to be incompressible and Newtonian, the left end of the airfoil to be fixed, and the structure to be of St. Venant- Kirchhoff (STVK) type.

Boundary Conditions

The boundary conditions are as follows:

- A constant parabolic inflow profile is prescribed at the left inlet as

$$v_f(0, y) = 1.5U_m \frac{4y(H - y)}{H^2}, \tag{11}$$

  where U_m is the mean inflow velocity and the maximum inflow velocity in $1.5U_m$
- At outlet, zero-stress $\sigma.n = 0$ is realized by using the 'do-nothing' approach in the variational formulation.
- Along the upper and lower boundary, the usual 'no-slip' condition is used for the velocity.
- Left end of airfoil is considered rigid.

Initial Conditions

The initial conditions are as follows:

$$v_f(t; 0, y) = \begin{cases} v_f(0, y)\frac{1-cos\left(\frac{\pi}{2}t\right)}{2}, & t < 2.0 \\ v_f(0, y), & t \geq 2.0 \end{cases} \tag{12}$$

NUMERICAL RESULTS: THE OBJECT ORIENTED PLATFORM 'DOpElib'

Software package: `DOpElib`

First, we introduce the software package that was used for C++ implementation. `DOpElib` is a modularized high-level algorithms toolbox based on the `deal.II` Finite Element Library. It was developed by Winnifried Wollner from University of Hamburg, Thomas Wick and Christian Goll from University of Heidelberg. Currently the software is in an early testing stage and not available. The main aims of `DOpElib` are following:

- Without any further work this software package enables researcher to implement only those moduls that are specific to their problem while being able to reuse other modules.

- DOpElib allows researcher to switch between different algorithms for the same problem with little effort because of the modularized access to the algorithms.
- To solve stationary and non-stationary PDE problems as well as optimal control problems constrained by PDEs.

The main features of DOpElib are:

- Researcher needs to provide only the problem specific data.
- There are various time stepping schemes, such as forward Euler, backward Euler, Crank-Nicolson, shifted Crank-Nicolson, and Fractional-Step-theta scheme.
- Goal-oriented error estimation.
- Mesh adaptation, etc.

For more details, we refer to [Goll, Wick and Wollner; Wick , 2011; Carraro, Goll and Marciniak-Czochra , 2013; Goll, Wick and Wollner , 2012; Richter and Wick , 2012].

Numerical Results

In this research, we introduce three FSI test cases that are treated with different inflow velocities (see Table-1) [8,9,10]. The parameters are chosen such that a visible transient behavior of the double wedge airfoil can be seen. To ensure a 'fair' comparison of results, we calculate the comparison values using the ALE method. For all cases, a uniform time-step size of $k = 0.0167s$ is used. But to ensure the convergence of numerical simulations, different time-step sizes and schemes are used and same result obtained.

Table 1: Parameter setting for the FSI test cases

Parameter	Test-1	Test-2	Test-3
Structure model	STVK	STVK	STVK
$\rho_f[kgm^{-3}]$	1000	1000	1000
$\rho_s[kgm^{-3}]$	2710	2710	2710
$\nu_f[m^{-2}s{-}1]$	1×10^{-3}	1×10^{-3}	1×10^{-3}
ν_s	0.33	0.33	0.33
$\mu_s[kgm^{-1}s^{-2}]$	68.9×10^6	68.9×10^6	68.9×10^6
$U_m[ms^{-1}]$	0.5	1.0	2.0

Table 2: Results for the test case 1, 2, and 3

	Test-1	Test-2	Test-3
DoF	83767808	83767808	331805056
$k[s]$	0.0167	0.0167	0.0167
$u_x(A)[\times 10^{-5}]$	0.1604	0.5078±0.061	2.675±4.973
$u_y(A)[\times 10^{-5}]$	0.5627	1.747±0.241	9.242±19.219
F_D	15.693	61.025±0.963	292.733±84.496
F_L	24.988	69.111±5.607	285.01±456.08
$\Delta P[\times 10^3]$	0.138	0.827±0.0295	6.306±2.462

The computed values of the FSI test-1,2 and 3 are summarized in the Table-2 and the velocity fields are displayed in Figure-8. The results of the FSI test-2 and 3 are displayed in the Figures-9 to 13. We begin with the FSI-1 test case. The time-dependent behavior of the deflections, Drag, Lift and pressure difference in between left end and right lower end of aerofoil became steady after $3.6s$. Displacement in the x and y direction became steady at 0.1604×10^{-5} and 0.5627×10^{-5}, respectively. We monitored a steady pressure difference (144.751), as well as the lift and drage force 24.988 and 15.693, respectively.

In FSI test case 2 and 3, the time-dependent behavior of the displacement, pressure difference, lift and drag force are not steady. We monitored an oscillation with a range of amplitude. In a simple sense we can

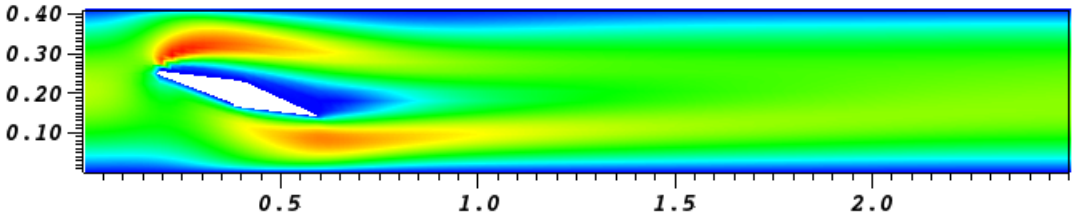

(a) Test-1

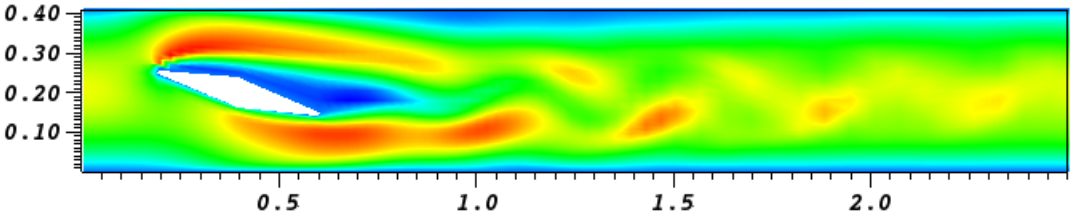

(b) Test-2

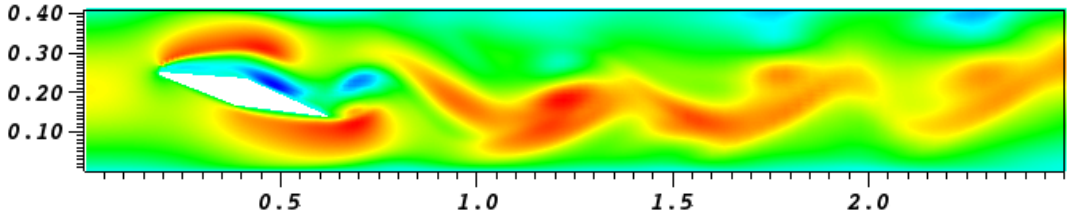

(c) Test-3

Figure 8: Velocity field

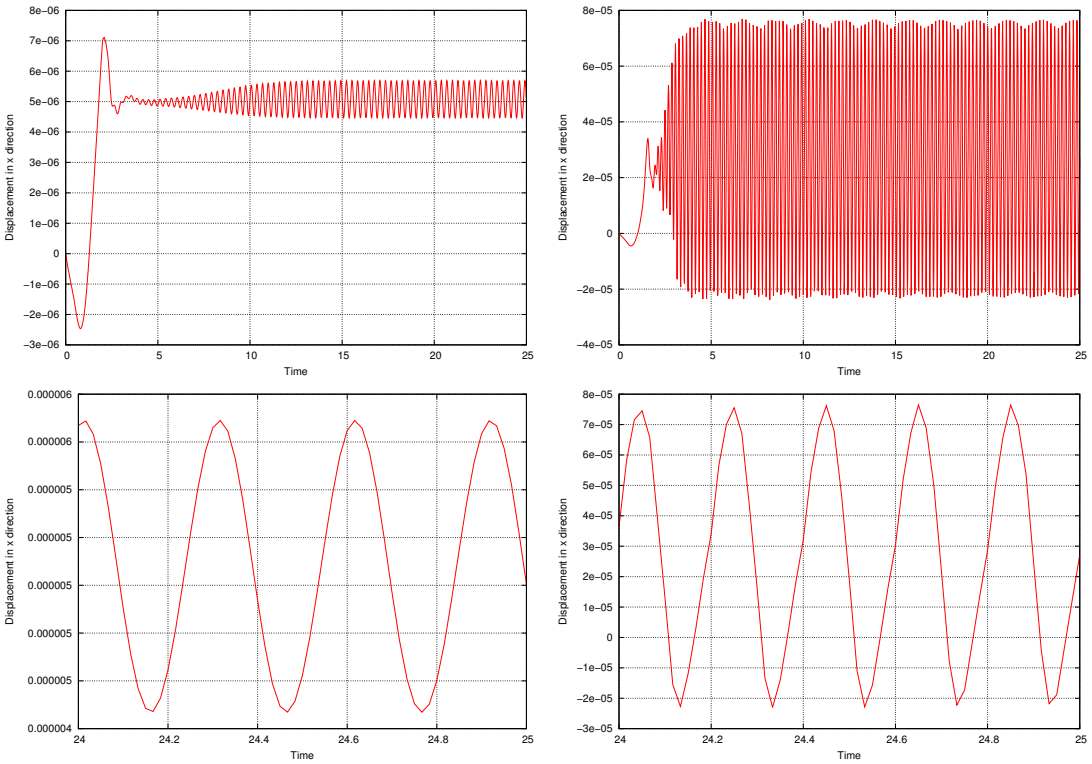

(a) Test-2

(b) Test-3

Figure 9: Displacement in x direction (u_x) of the control point $A(t)$

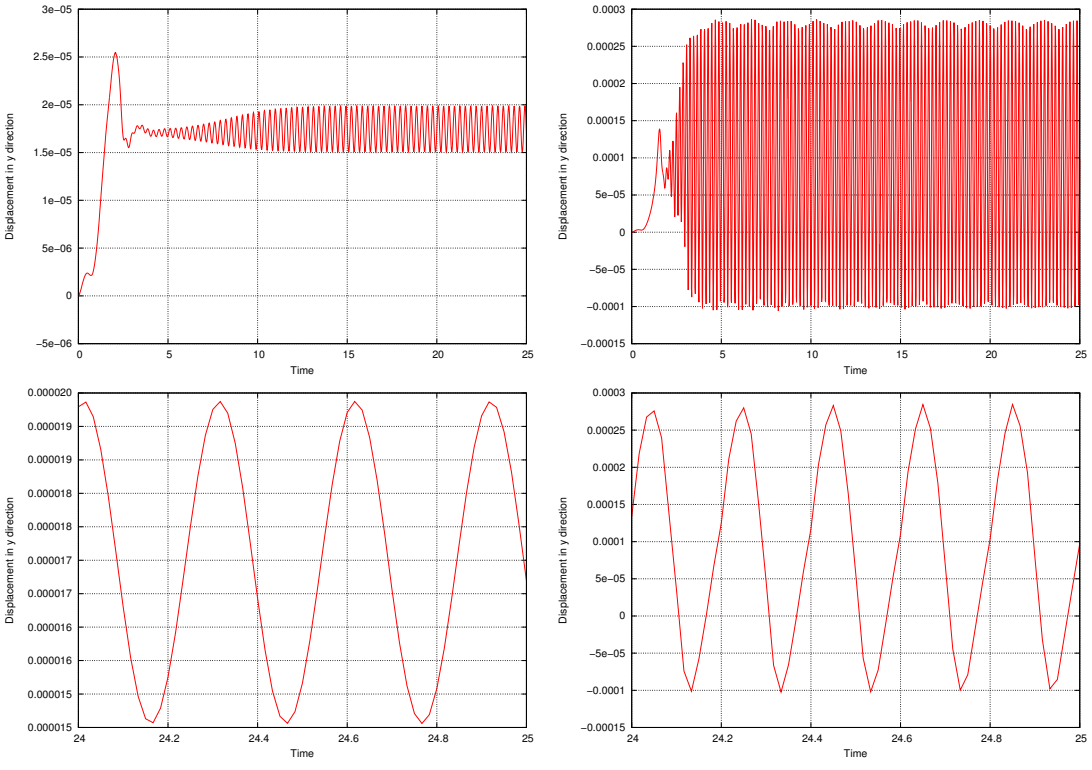

(a) Test-2 (b) Test-3

Figure 10: Displacement in y direction (u_y) of the control point $A(t)$

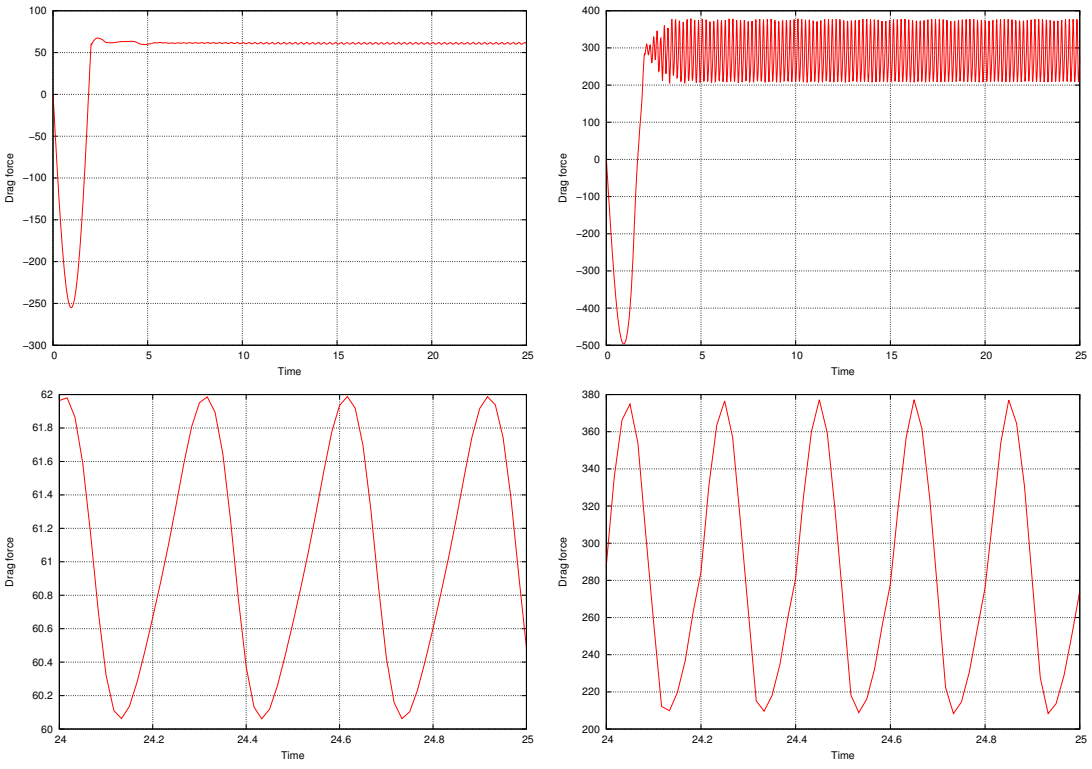

(a) Test-2 (b) Test-3

Figure 11: Variation of drag force (F_D) over time

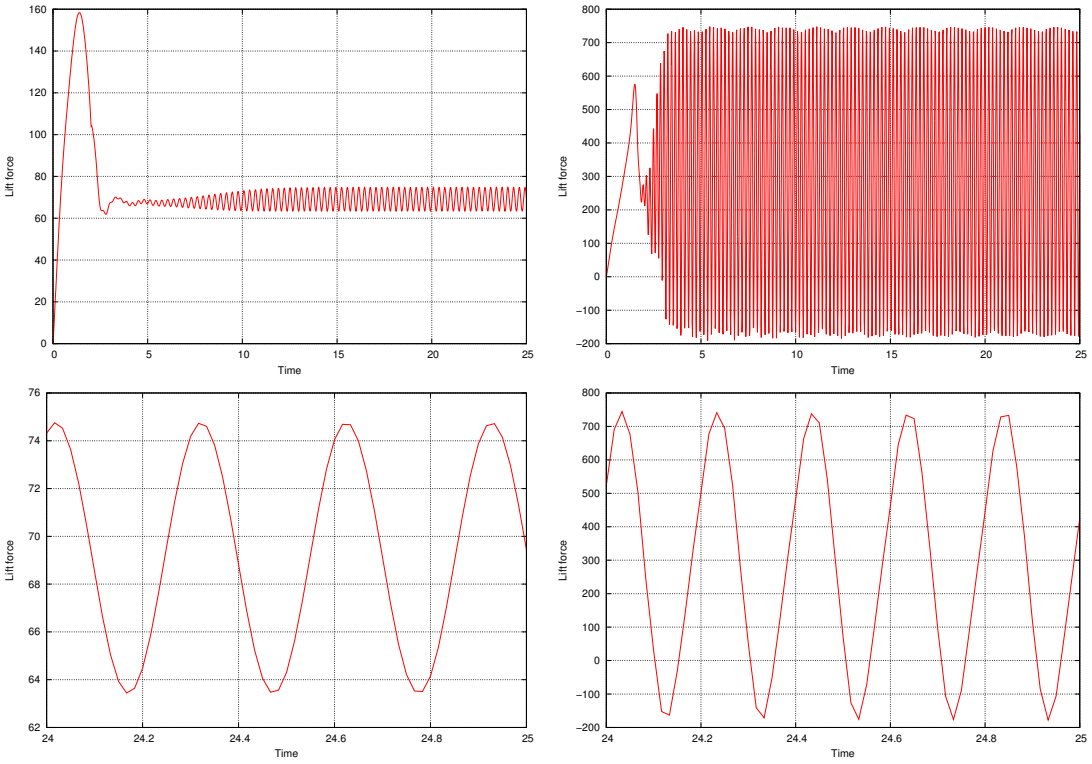

(a) Test-2 (b) Test-3

Figure 12: Variation of lift force (F_L) over time

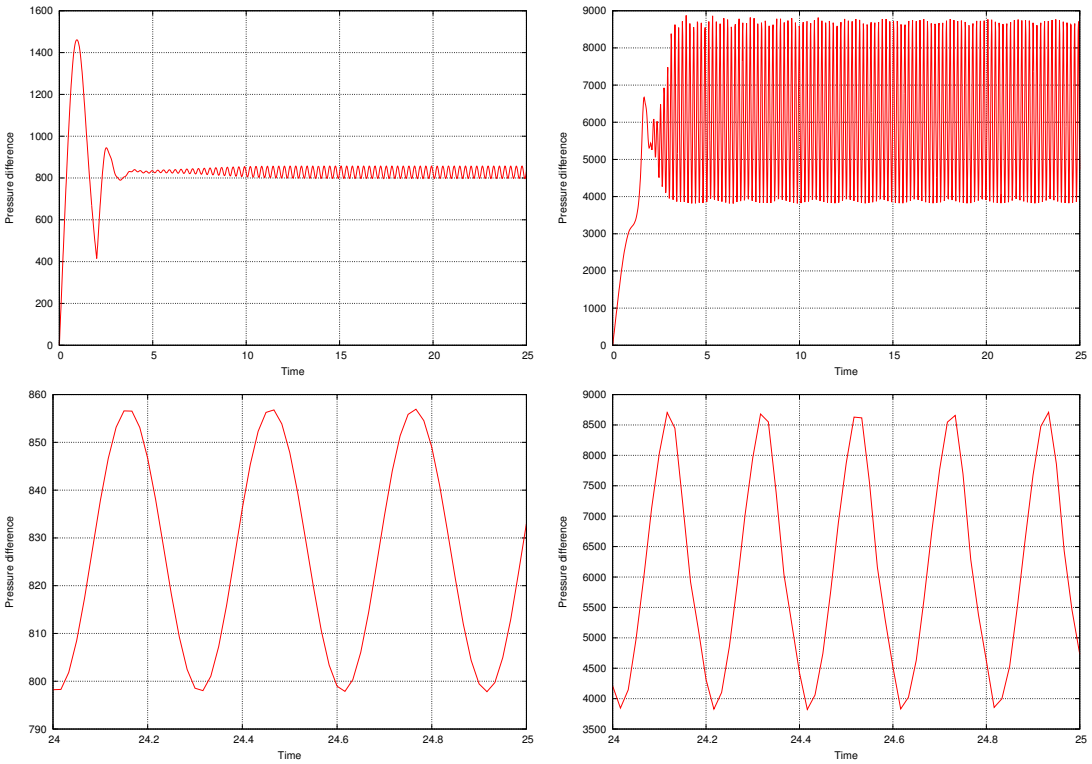

(a) Test-2 (b) Test-3

Figure 13: Pressure difference (ΔP) between leading and trailing edge

say that vibration is an oscillatory motion of a mechanical dynamic system or structure around same reference state, which is often the state of static equilibrium. In fact vibrations often are undesirable in mechanical structures as they cause fatigue failure and lead to increase of stress and bearing loads etc. For example, if an aircraft wing vibrates excessively, especially with the frequencies in the range of the natural frequencies (approx. $4-8\ Hz$) of the human body and organs, passengers inside the aircraft will feel uncomfortable and it can cause serious internal trauma (Leatherwood and Dempsey, 1976 NASA TN D-8188). But if aircraft wings vibrate with large amplitudes for an extended period of time, there will be fatigue failure in wings, which would potentially cause the aircraft to crash with massive fatalities. The Tacoma Narrows Bridge disaster in 1940 was one of the most famous engineering disasters of all time, and it failed due to the same type of self-excited vibration behavior that occurs in aircraft wings.

CONCLUSIONS

This project is focused on computing prototype configurations to test the code, which will help us to use the software to computing any realistic applications. The numerical simulations FSI on a sample aircraft wing (3D) still under test. This paper mainly deal with a double wedge airfoil ($2D$), where the left end of this airfoil is considered rigid and the control points $A(t)$ are fixed at the trailing edge with $A(t)|_{t=0} = (0.6, 0.147)$. We observed different behaviors of the double wedge airfoil with different FSI test cases. In test cases FSI-1, the deflection of trailing edge of the airfoil became steady, while in FSI test-2 and 3, we observed oscillating behavior. Therefore, we conclude that the deflective behavior of structures becomes unsteady under high-speed fluid flow, which can be cause of massive fatalities.

References

T. Richter (2012), *A Fully Eulerian Formulation for Fluid-Structure-Interaction Problems*, Institute for Applied Mathematics, University of Heidelberg, Germany, 2012.

T. Wick (2011), *Adaptive Finite Elements for Monolithic Fluid-Structure Interaction on a Prolongated Domain: Applied to an Heart Valve Simulation*, Computer Methods in Mechanics, Warsaw, Poland, 2011.

W. Wollner (2011), *Optimization of Complex System*, University of Hamburg, 2011.

T. Dunne (2007), *Adaptive Finite Element Approximation of Fluid-Structure Interaction Based on Eulerian and Arbitrary Lagrangian-Eulerian Variational Formulations*, Doctoral Report, Institute for Applied Mathematics, University of Heidelberg, Germany, 2007.

M. Hinze (2011), *Numerical Methods for PDEs Finite Elements*, Department of Mathematics, University of Hamburg, 2011.

T. Richter (2010), *Numerical Methods for Fluid-Structure Interaction Problems*, Institute for Applied Mathematics, University of Heidelberg, Germany, 2010.

T. Dunne (2009), *Adaptive Finite Element Simulation of Fluid Structure Interaction Based on Monolithic Variational Formulations*, Institute for Applied Mathematics, University of Heidelberg, Germany, 2009.

J. Struckmeier (2012), *Advanced Fluid Dynamics: Lecture Notes on Advanced Fluid Dynamics*, University of Hamburg, 2012.

T. Richter and R. Rannacher (2010), *Adaptive finite element simulation of fluid- structure interaction based on a Fully Eulerian variational formulation*, Fluid-Structure Interaction II: Modelling, Simulation, Optimisation, Springer, Vol. 73, 1st Ed., pp 159-191, 2010.

W. Bangerth, T. Heister and G. Kanschat, *`deal.II` Differential Equations Analysis Library*, web: www.dealii.org

C. Goll, T. Wick and W. Wollner, *`DOpElib`: The `deal.II` based optimization library*, web: www.dopelib.uni-hamburg.de

T. Dunne and R. Rannacher (2006), *Adaptive Finite Element Simulation of Fluid Structure Interaction Based on an Eulerian Formulation*, Fluid-Structure Interaction: Modelling, Simulation, Optimisation, Springer, Vol. 53, pp 110-145, 2006.

G. P. Galdi and R. Rannacher (2010), *Fundamental Trends In Fluid-Structure Interaction, Contemporary Challenges in Mathematical Fluid Dynamics and its Applications*, World Scientific Publishing Co. Pte. Ltd., Vol. 1, 2010.

S. Boenisch (2007), *Adaptive Finite Element Methods for Rigid Particulate Flow Problems*, Doctoral Report, Institute for Applied Mathematics, University of Heidelberg, Germany, 2007.

T. Carraro and C.Goll (2013), A. Marciniak-Czochra, A. Mikelic, *Pressure jump interface law for the Stokes-Darcy coupling: Confirmation by direct numerical simulations*, Journal of Fluid Mechanics, submitted, 2013.

C. Goll, T. Wick and W. Wollner (2012), *DOpElib: Differential Equations and Optimization Environment; A Goal Oriented Software Library for Solving PDEs and Optimization Problems with PDEs*, ACM Transactions on Mathematical Software, submitted, 2012.

T. Richter and T. Wick (2012), *Optimal Control and Parameter Estimation for Stationary Fluid-Structure Interaction Problems*, Heidelberg University, submitted, 2012.

Bungartz, H. J. and Schaefer, M. (Eds.). *Fluid-Structure Interaction*. Springer, 2006.

Bungartz, H. J., Miriam M. and Schaefer, M. (Eds.) (2010). *Fluid-Structure Interaction-II*. Springer, 2010.

Bangerth, W. and Rannacher, R. (2003). *Adaptive Finite Element Methods for Differential Equations*. Springer, 2003.

Ebna Hai, B.S.M. and Bause, M. (2013). *Adaptive Multigrid Methods for Fluid-Structure Interaction (FSI) Optimization in an Aircraft and design of integrated Structural Health Monitoring (SHM) Systems"*. 2nd ECCOMAS Young Investigators Conference (YIC2013), Bordeaux, France (Accepted).

ACKNOWLEDGMENT

Thanks go to W. Wollner, T. Wick and C. Goll for developing the wonderful software packages `DOpElib`.